Electronic Supplementary Material (ESI) for Soft Matter.

Supplementary Material

Anionic starch-based hybrid cryogels embedded ZnO nanoparticles: tuning the elasticity and pH-functionality of biocomposites with dicarboxylic acid units

Sena CİFTBUDAK[a] and Nermin ORAKDOGEN[b*]

[a]Graduate School of Science Engineering and Technology, Department of Chemistry, Istanbul Technical University, 34469, Maslak, Istanbul, Turkey

[b]Istanbul Technical University, Department of Chemistry, Soft Materials Research Laboratory,

34469, Maslak, Istanbul, Turkey.

*Correspondence to: Prof. Nermin Orakdogen (e-mail: *orakdogen@itu.edu.tr*), Phone: 0090-212-2853305.

Structural characterization of semi-IPN biocomposites

Table S1. Characteristic functional group assignments of raw starch (ST).

Peak Appearance Wavelength	
Characteristic Functional Group Assignments	**ST (cm^{-1})**
C-O bending associated with the OH group	1646
C-H symmetrical scissoring of CH2OH moiety	1421
C - O - C asymmetric stretching	1154
C - O - C ring vibration of carbohydrate	925, 852
C - O stretching	1086
CH2 symmetric deformation and scissoring	1414-1451
C -H symmetric bending	1363

Network characteristics of semi-IPN biocomposites

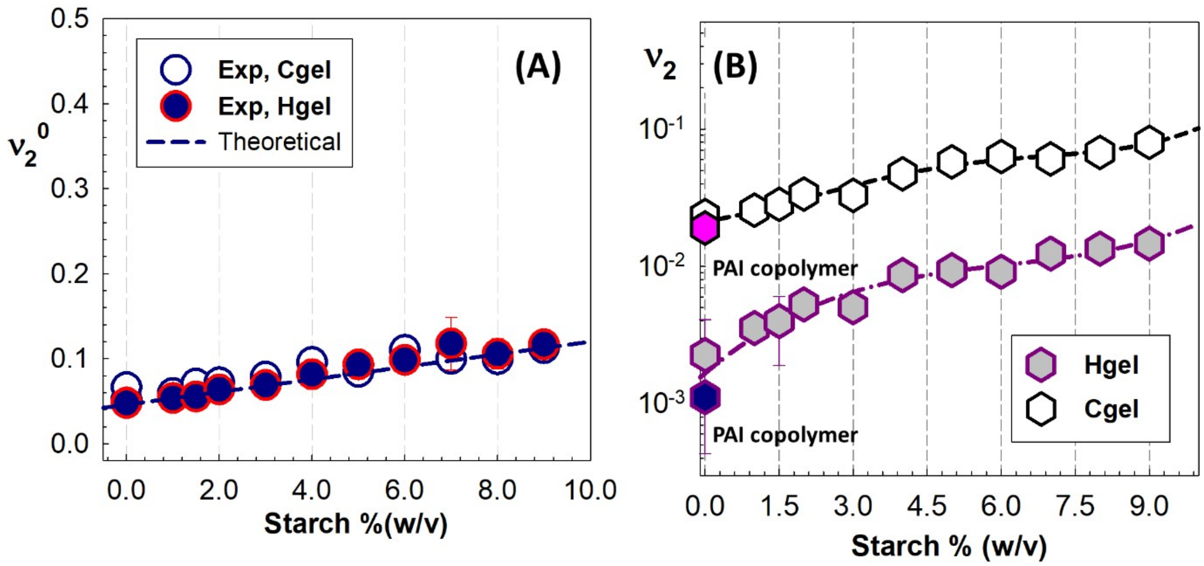

Figure S1. Network characteristics of semi-IPN biocomposites. (A) Experimental and theoretical ν_2^0 values, (B) volume fraction of crosslinked polymer in the swollen network of ST-PAI/ZnO gels shown as a function of ST concentration.

Elasticity of starch blended ZnO-embedded biocomposites

Figure S2 shows the stress-strain curves of ST-PAI/ZnO Hgels from the uniaxial compression tests after preparation-state (A), after swollen-state (B) and stress-strain curves of ST-PAI/ZnO Cgels after swelling (C). Snapshots during finger compression of ST1-PAI/ZnO Hgel sample containing 1.0% (w/v) of starch in the feed (D).

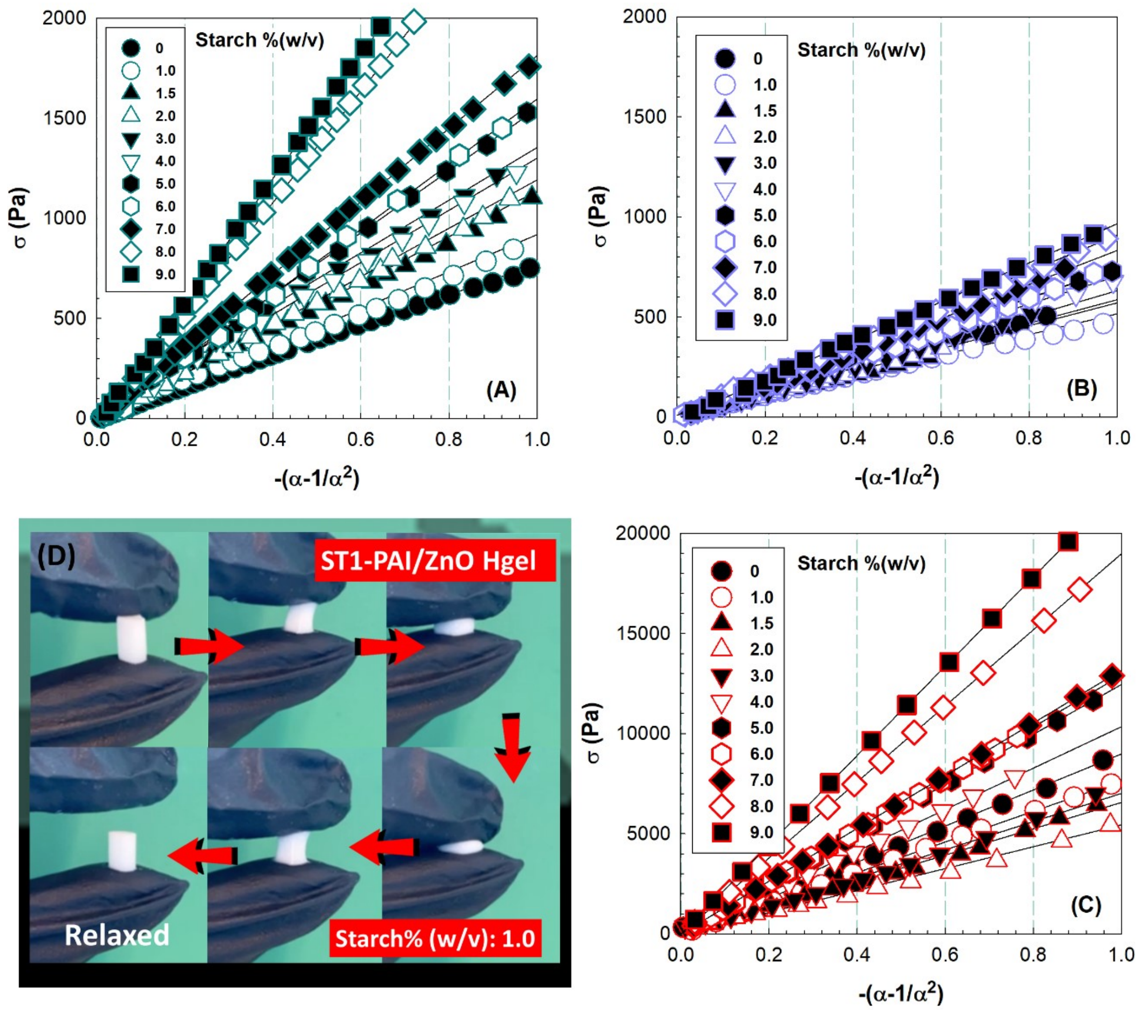

Figure S2. Stress-strain curves of ST-PAI/ZnO Hgels from the uniaxial compression tests after preparation-state (A), after swollen-state (B) and stress-strain curves of ST-PAI/ZnO Cgels after swelling (C). Snapshots during finger compression of ST1-PAI/ZnO Hgel sample containing 1.0% (w/v) of starch in the feed (D).

Figure S3 compares the optical appearances of ST-PAI/ZnO hydrogel and cryogel samples containing 1.5% and 7%(w/v) starch in the feed during uniaxial compression.

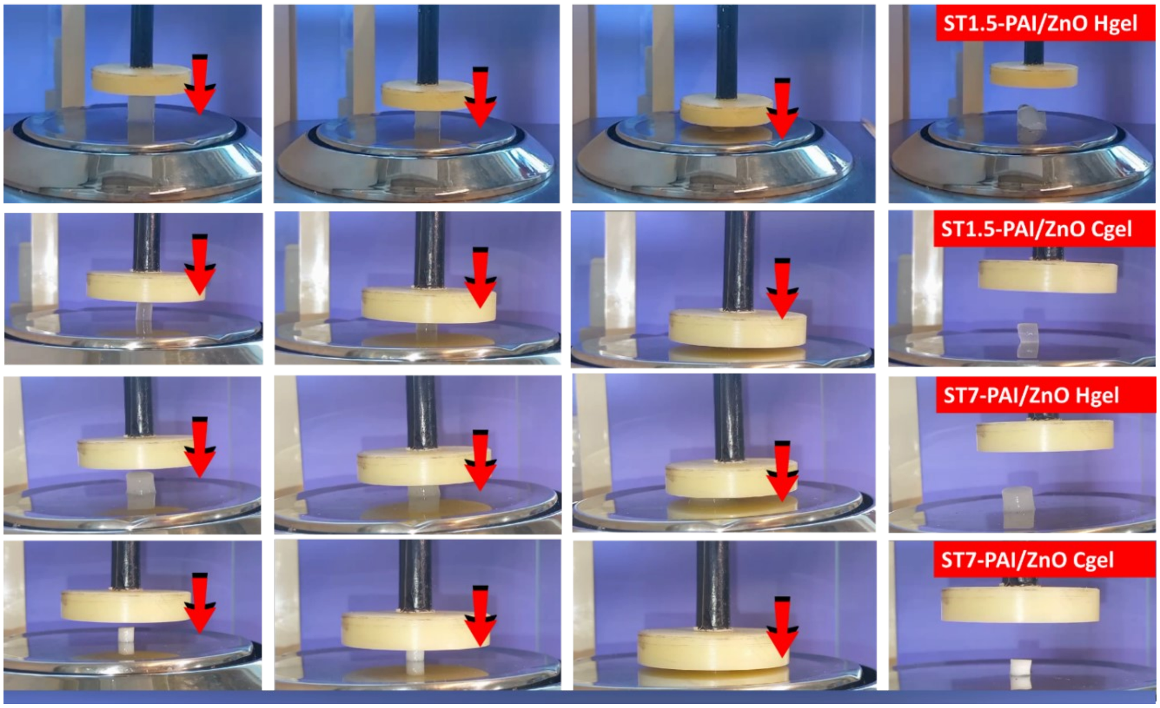

Figure S3. Optical appearances of ST-PAI/ZnO hydrogel and cryogel samples containing 1.5% and 7%(w/v) starch in the feed during uniaxial compression.

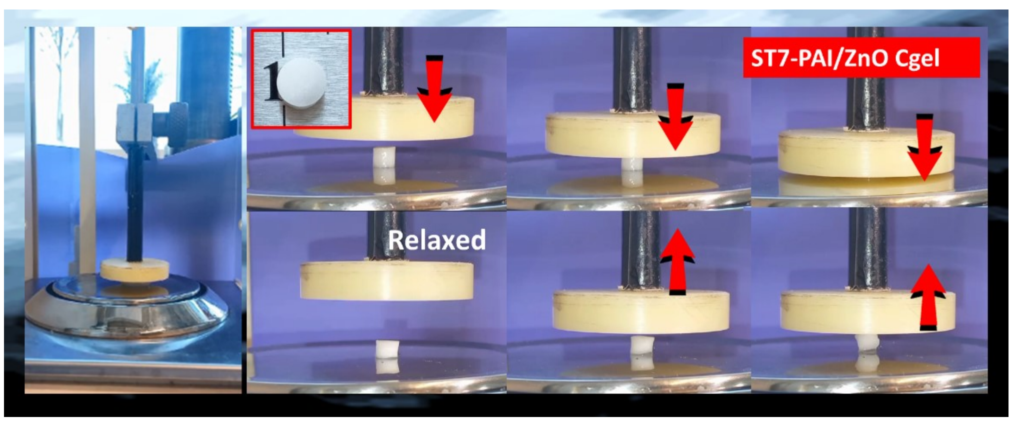

Figure S4. Optical appearances of ST7-PAI/ZnO Cgel sample containing 7%(w/v) in the feed during uniaxial compression.

pH-induced swelling of starch blended ZnO-embedded biocomposites

Figure S5 shows pH-sensitive swelling results in order of increasing pH as well as starch content in the feed for ST-PAI/ZnO Hgels. Figure S3 presents the variation of $\ln \varphi(t)/\varphi_W$ versus ln*t*, and the water fraction $\varphi(t)/\varphi_W$ versus $t^{1/2}$ curves of semi-IPN ST-PAI/ZnO Hgels with different starch content in pH 11.2 solution.

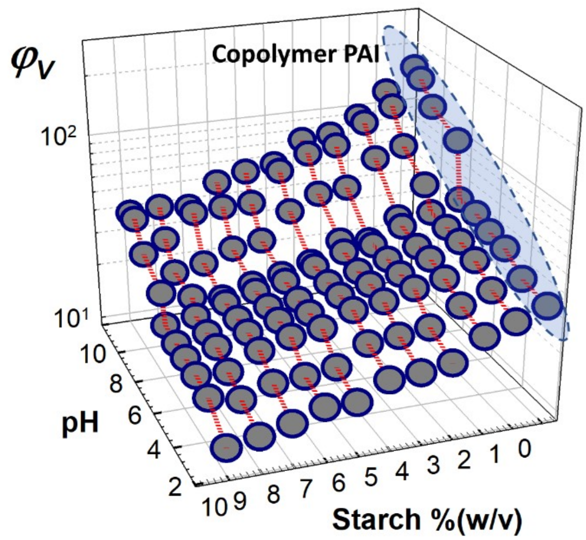

Figure S5. pH-sensitive swelling results in order of increasing pH as well as starch content in the feed for ST-PAI/ZnO Hgels.

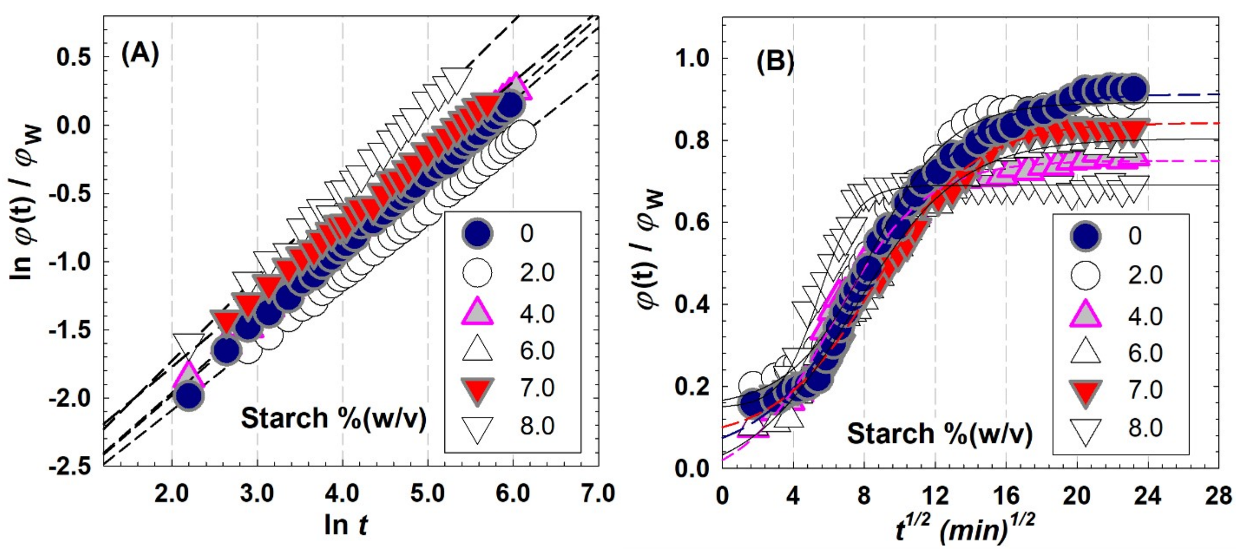

Figure S6. (A) Variation of $\ln \varphi(t)/\varphi_W$ versus ln*t*, and (B) water fraction $\varphi(t)/\varphi_{\mathrm{W}}$ versus $t^{1/2}$ curves of semi-IPN ST-PAI/ZnO Hgels with different starch content in pH 11.2 solution.

Salt-induced swelling of starch blended ZnO-embedded biocomposites

Figure S7 shows the swelling of ST-PAI/ZnO Cgels with various starch content in the presence of different salts: NaBr, NaCl, $NaNO_3$ and Na_2SO_4.

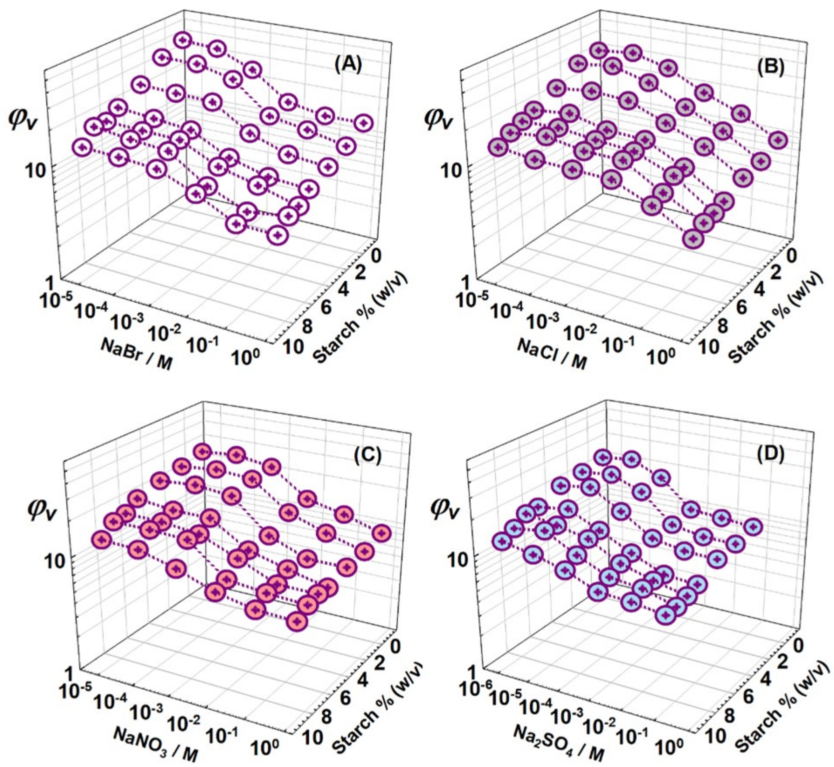

Figure S7. Swelling of ST-PAI/ZnO Cgels with various starch content in the presence of different salts: NaBr (A), NaCl (B), $NaNO_3$ (C) and Na_2SO_4 (D).

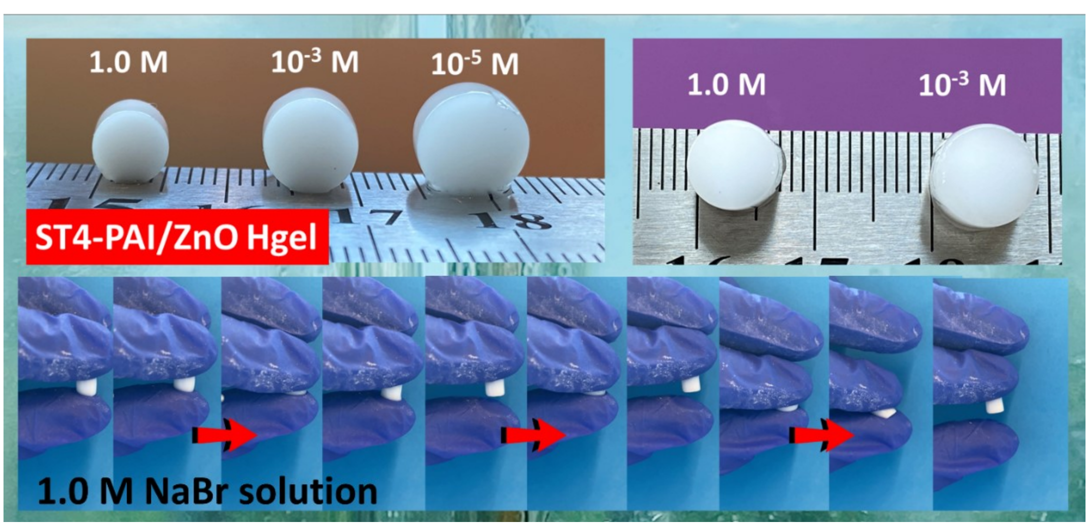

Figure S8. Optical appearances of ST4-PAI/ZnO Hgel sample containing 4.0 %(w/v) starch after swelling in NaBr solutions of different ionic strength. Mechanical stability of the sample after swelling in 1.0 M of NaBr solution.

Adsorption capacity of semi-IPN biocomposites for MV dye

Table S2. Kinetic parameters describing the adsorption of MV onto semi-IPN ST-PAI/ZnO Hgels prepared at different starch content based on pseudo-first-order, pseudo-second-order, Elovich, and intraparticle diffusion models.

	Pseudo-first order model		Elovich model		
Starch %(w/v)	$k_1 \times 10^{-2}$ (min^{-1})	R^2	α (mg/g min)	β (g/mg)	R^2
0	1.8143	0.9322	7.3985	0.3330	0.9825
8.0	3.5223	0.8568	2.4000	0.6680	0.9116
9.0	4.265128	0.8704	1.7388	0.7236	0.9308

	Pseudo-second order model		Intraparticle diffusion model			
Starch %(w/v)	$k_2 \times 10^{-2}$ (min^{-1})	R^2	$k_{initial}$ (mg g^{-1} min$^{-1/2}$)	R^2	k_{later} (mg g^{-1} min$^{-1/2}$)	R^2
0	0.6042	0.9948	3.2861	0.9926	0.7518	0.9857
8.0	1.7327	0.9970	2.1930	0.9669	0.4728	0.7075
9.0	1.4957	0.9967	1.8384	0.9687	0.2020	0.8780

Table S3. Thermodynamic parameters for adsorption of MV dye and adsorption capacity of semi-IPN ST-PAI/ZnO Cgels and Hgels prepared at different starch content calculated from various kinetic models.

	ST-PAI/ZnO Cgels				**ST-PAI/ZnO Hgels**			
Starch %(w/v)	Exp. q_e (mg/g)	Pseudo-first order q_{e1} (mg/g)	Pseudo-second order q_{e2} (mg/g)	ΔG^o (J/mol K)	Exp. q_e (mg/g)	Pseudo-first order q_{e1} (mg/g)	Pseudo-second order q_{e2} (mg/g)	ΔG^o (J/mol K)
0	12.230	8.715	12.727	-2533.7	18.556	11.455	17.963	-5192.9
8.0	5.719	4.009	6.092	-1307.4	7.552	5.054	7.747	-1108.1
9.0	8.397	5.264	8.763	-1835.8	6.635	5.264	7.015	-975.3